

# Aggregation Phenomena in AgX Precipitation in the Presence of Gelatin

M. G. Antoniadis and J. S. Wey\*

Manufacturing Research and Engineering Organization, Eastman Kodak Company, Rochester, New York

Despite the continuous development of new synthetic polymers, gelatin remains as the principal component of the binder used in most silver halide photographic films and papers. The main reason for the longevity of gelatin in silver halide photographic systems is its remarkable property to play a unique role in almost every step of the manufacture as well as in the photographic processing of these products. The most important function of gelatin in the preparation of photographic emulsions is to provide colloid protection and stabilization for the AgX crystals. Colloid stability of fine AgX particles is provided through steric stabilization, facilitated by the adsorption of gelatin on the AgX surface. A critical level of gelatin is required for such stabilization. The experimentally estimated critical gelatin surface coverage required to prevent coalescence during precipitation is in good agreement with previous theoretical calculations and with equilibrium adsorption measurements. Inadequate peptization of AgX colloid particles during precipitation can cause aggregation that can lead to undesirable agglomeration and coalescence. But in some cases gelatin can attenuate flocculation and control coalescence resulting in desirable dislocations such as the formation of twinning dislocations, which is the key step in the nucleation and growth of tabular AgX crystals. This is demonstrated by a strong correlation between the degree of flocculation during nucleation and the resulting tabular grain population fraction.

Journal of Imaging Science and Technology 42: 393–398 (1998)

## Introduction

The formation of silver halide microcrystals in the presence of gelatin is affected by a host of variables.<sup>1</sup> Although fundamental mechanisms of formation are not completely understood, it is known that in double-jet precipitation a stable number of nuclei is formed initially and, under controlled conditions, remains constant throughout the precipitation. Leubner, Jagannathan, and Wey<sup>2</sup> developed a dynamic mass balance model for determining the number of stable nuclei formed during the nucleation step of double-jet precipitation of AgBr crystals in the presence of gelatin. This model is in good agreement with experimental results except under some conditions that showed a decrease in the number of nuclei produced with increasing reactant addition rate. This anomaly was attributed to coalescence. Therefore, the understanding of aggregation phenomena in silver halide precipitation is very pertinent. The importance of agglomeration in the nucleation and growth of silver halide crystals has been stressed by other researchers.<sup>3–5</sup>

In this discussion the terms “aggregation” and “agglomeration” are used generically, whereas the terms “flocculation” and “coalescence” are used to designate specific events. *Flocculation* refers to loosely held aggregates of noncontacting colloidal particles. In this case, the attraction forces are almost counterbalanced by the repulsion forces, thus preventing particle contact. *Coalescence*, refers to the event by which two or more single crystalline particles combine to form a new, larger crystalline particle.

In most silver-based photographic applications, silver halide crystals are peptized by gelatin, which, through surface adsorption, provides steric stabilization. However, under certain precipitation conditions inadequate levels of gelatin may be available for peptization, and some agglomeration can occur. In this presentation we shall review the conditions that cause such phenomena to take place and discuss their consequences.

## Part I. Determination of Critical Gelatin Level

A well-mixed continuous crystallizer operating at steady state and with a short residence time provides a suitable environment for studying the factors affecting the agglomeration of fine silver halide particles under controlled conditions. In this case, the particle size in the reactor effluent can be measured and the presence of agglomeration determined at different steady state conditions.

**Experimental.** The continuous reactor used comprised a cylindrical cavity with a center-mounted turbine. The reactants (gelatin, NaBr, and AgNO<sub>3</sub>) were added through three inlet ports, and the mixed suspension was removed through an exit port. The volume of the reactor was 33.7 mL. Residence time distribution analysis indicated that the reactor contents were well mixed.

The reactor was operated with an average residence time of 1.7 sec. The flow rates of the reactants were 16.7 mL/sec for the gelatin solution and 1.67 mL/sec for the NaBr and AgNO<sub>3</sub> solutions. The concentration of the gelatin reactant solution determined the average gelatin concentration in the reactor at steady state, and the AgNO<sub>3</sub> reactant concentration determined the steady state AgBr suspension density in the reactor. The gelatin used was a deionized, lime-processed, ossein gelatin with an isoelectric point of 4.9. The pBr of the effluent was measured potentiometrically, using a Ag/AgBr electrode, and the desired

Original manuscript received March 16, 1998.

\* IS&T Fellow

© 1998, IS&T—The Society for Imaging Science and Technology

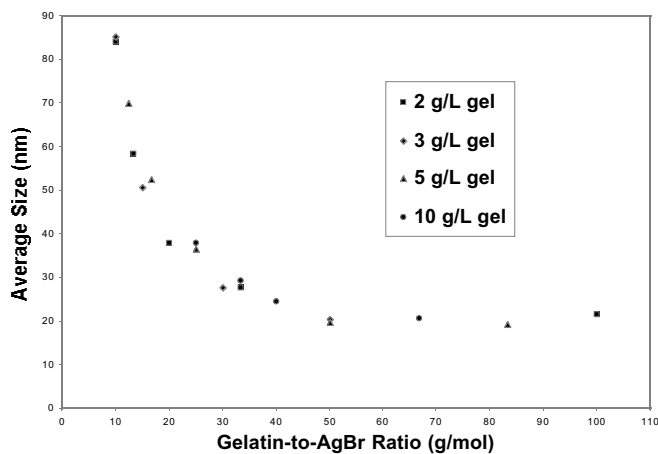


**Figure 1.** Average particle diameter of single particles, obtained by deflocculation, as a function of gelatin-to-AgBr ratio in a continuous reactor.

pBr was obtained by adjusting the concentration of the NaBr reagent. The temperature of the reactor effluent was controlled by adjusting the temperature of the reactants.

The size of the single particles and aggregates formed in the reactor was determined by an in-line turbidity measurement of the reactor effluent as described in Ref. 6. The average size of the single particles was obtained by turbidimetry and dynamic light scattering (DLS) measurements after withdrawing samples from the reactor effluent and quenching them using 4-hydroxy-6-methyl-1,3,3a,7-tetraazaindene (TAI) as described in Ref. 6. The discrepancy between the sizes obtained by turbidity and DLS was in most cases smaller than 15%, with the DLS measurements yielding the larger size as expected.<sup>6</sup> The sizes reported below are the averages of these two measurements.

**Results and Discussion.** The in-line turbidity measurements indicated that the particles were flocculated in most cases. Flocculation was inferred by the difference between the effective particle size measured by the in-line measurements and the size obtained after quenching with TAI. The degree of flocculation as indicated by this difference increased as the gelatin level decreased. Hence, deflocculation with TAI was necessary to obtain the size of the single particles.

The primary variables affecting the size of the deflocculated crystals were the average gelatin concentration,  $c_g$ , and the AgBr suspension density,  $c_s$ , in the continuous reactor at steady state. Good correlation was obtained between the particle size and the ratio of these two parameters, hereinafter denoted by  $R_{gs}$  and referred to as the gelatin-to-AgBr ratio. The effect of this variable on the particle size at a steady state of pBr 2.3, pH 4.5, and 40°C is shown in Fig. 1. The range of gelatin concentrations in these experiments was 2 to 10 g/L, and the AgBr suspension density was varied from 0.02 to 0.4 mol/L. The effects of pBr, temperature, and pH were found to be secondary compared to the effect of the gelatin-to-AgBr ratio.

As seen from Fig. 1 the particle size is independent of the gelatin-to-AgBr ratio above a value of about 50 g/mol but increases sharply below this value. These results reveal the importance of the amount of gelatin available for adsorption on the AgBr particles and suggest an inverse relationship between the gelatin-to-AgBr ratio and the particle size for ratios below 50 g/mol. This relationship is elucidated by derivation of an expression for the amount of gelatin

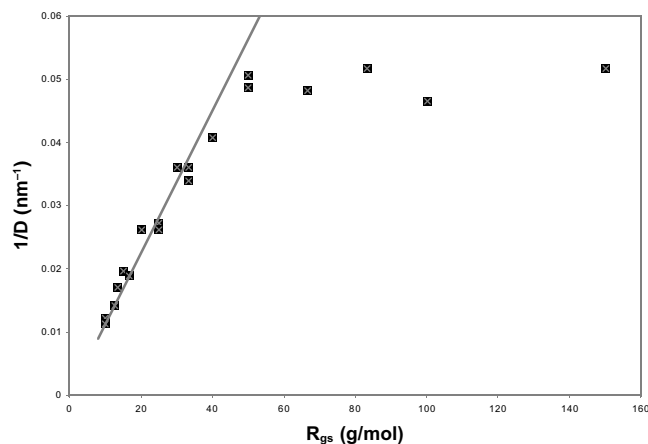


**Figure 2.** Plot of  $1/D$  of single particles, obtained by deflocculation, versus  $R_{gs}$  in a continuous reactor. The solid line is a linear regression for  $R_{gs}$  values below 40 g/mol.

adsorbed per unit surface area of the AgBr particles,  $M$ , through the division of the mass of adsorbed gelatin per reactor volume,  $\Phi c_g$ , by the AgBr surface area per reactor volume,  $(c_s W/\rho)(6/D)$ , where  $\Phi$  is the mass fraction of gelatin adsorbed,  $c_g$  and  $c_s$  are defined above,  $W$  is the molecular weight of AgBr,  $\rho$  is the crystal density and  $6/D$  is the surface-to-volume ratio. The final expression for  $M$  becomes

$$M = \frac{\Phi R_{gs} \rho D}{6W}, \quad (1)$$

where  $R_{gs}(=c_g/c_s)$  is the gelatin-to-AgBr ratio. Rearranging this equation gives

$$1/D = \frac{\rho/6W}{M/\Phi} R_{gs}, \quad (2)$$

which indicates that, if  $M/\Phi$  is constant,  $R_{gs}$  is inversely proportional to  $D$  and a plot of  $1/D$  versus  $R_{gs}$  should yield a straight line passing through the origin.

Figure 2 shows a plot of  $1/D$  versus  $R_{gs}$  for the data of Fig. 1, where  $D$  is the average of the mean diameters measured by turbidity and DLS. This figure demonstrates that the relationship between  $R_{gs}$  and this inverse diameter is indeed linear below an  $R_{gs}$  value of 50 g/mol. The correlation coefficient obtained for  $R_{gs}$  values below 40 g/mol and by forcing the line through the origin is 0.97. Therefore, an upper limit of the gelatin coverage,  $M$ , may be calculated from the slope of the regression line. The calculated upper limit of 5.1 mg/m<sup>2</sup> is in good agreement with the previously measured saturation coverage<sup>7</sup> (5 to 8 mg/m<sup>2</sup>), considering that lower values than the saturation coverage may be adequate for stabilization, and with the theoretical calculation of the minimum thickness of adsorbed gelatin necessary to constrain aggregation of fine silver halide grains.<sup>8</sup>

The dramatic increase in the size of single, deflocculated particles at gelatin levels below 50 g/mol shown in Figs. 1 and 2 must be a result of irreversible aggregation because diffusion mechanisms cannot account for the fast growth rates required to achieve such sizes at the residence time used. Furthermore, x-ray diffraction indicated that the aggregated particles were monocrystalline. It is, therefore, concluded that the irreversible aggregation revealed by these experiments is caused by coalescence. This conclusion is supported by electron microscopy.<sup>6</sup> Coalescence occurs because at low gelatin-to-AgBr ratios

the amount of gelatin available is not sufficient to stabilize the small nuclei formed in the reactor. However, as the particle size increases through coalescence, the total surface area decreases until the available gelatin is adequate for stabilization. It is assumed that all these events occur within the average residence time of the reactor. The linear relationship between  $R_{gs}$  and the inverse size can thus be viewed as a correlation between the total available gelatin and the total surface area of the stable suspension.

## Part II. Coalescence in Double-Jet Nucleation

Although the continuous crystallizer is well suited for the determination of the critical gelatin level for stabilizing AgX microcrystals, the double-jet precipitation is a more commonly used process. As discussed in the *Introduction* section, a model for the determination of the number of stable crystals formed in double-jet nucleation has been developed. The consequences of agglomeration in this process are further discussed below.

**Experimental.** The precipitation experiments were conducted by the balanced double-jet addition of  $\text{AgNO}_3$  and  $\text{NaBr}$  to a gelatin-containing solution agitated by a center-mounted radial-flow mixer. The two reactant solutions were added to the well-mixed gelatin solution through separate subsurface introduction close to the mixer. This addition allowed the reactant streams to be diluted immediately by the circulating bulk suspension containing the gelatin.

In each experiment 100 mL of  $\text{AgNO}_3$  and 100 mL of  $\text{NaBr}$  solutions were added at the same constant flow rate, by the procedure described above, to a gelatin solution that was at a specified concentration, temperature, pBr, and pH. By changing the constant flow rate of the reactants, their molar addition rate per unit suspension volume,  $R$ , could be varied while the total mass of AgBr precipitated remained the same. The  $\text{NaBr}$  solutions were at a concentration needed to maintain pBr, which was measured potentiometrically, at its initial value. Constant temperature was also maintained. The size of the AgBr crystals produced during the precipitation experiments was obtained by turbidimetry, and the number of crystals per unit suspension volume,  $Z$ , was calculated from the size using a mass balance, as described in Ref. 9.

In a typical experiment, the turbidity was measured in-line during the precipitation at a specified gelatin concentration, pBr, pH, and  $R$ , by circulating a portion of the reaction vessel contents, at high flow rate through a turbidimeter, providing a transient crystal size and crystal number.<sup>9</sup> At the end of the precipitation, a small sample was withdrawn from the reactor vessel and quenched with TAI, which readily deflocculated the crystals (if they were flocculated) and greatly restrained Ostwald ripening. The turbidity of the quenched sample was then measured and the particle size and number calculated. The difference between the in-line measurements and the measurements after quenching with TAI was an indicator of the presence and the degree of flocculation.

**Results and Discussion.** According to the model of Ref. 2, the stable number of crystals,  $Z$ , formed during double-jet nucleation at high gelatin concentration, constant temperature, and controlled pBr increases with increasing reactant addition rate,  $R$ , and the slope of  $\log Z$  versus  $\log R$  is less than unity. In addition, this model predicts that  $Z$  increases with decreasing AgBr solubility (e.g., decreasing temperature). These predictions were verified in this

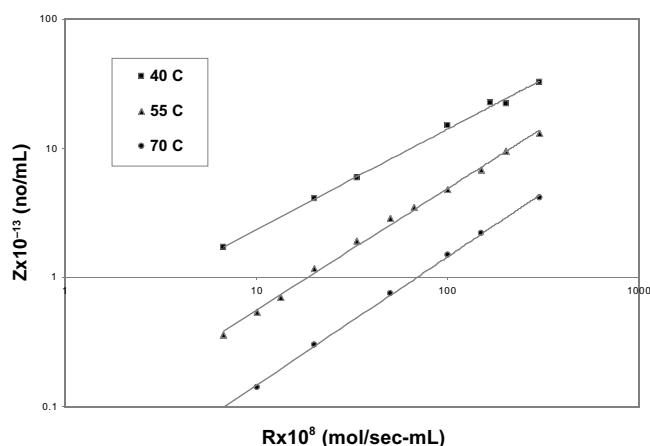


**Figure 3.** Plots of  $Z$  versus  $R$  obtained by double-jet precipitation at three temperatures in the presence of high-gelatin concentration. The lines represent linear regressions.

study at several pBr and temperature conditions. The initial volume and the concentration of the reactants did not significantly affect these results. These observations indicate that mixing was not a limiting factor at the conditions used in these experiments.

Typical plots of  $\log Z$  versus  $\log R$  are shown in Fig. 3 at three temperatures, pBr 2.3 (at 40°C), pBr 2.2 (at 55°C), pBr 2.0 (at 70°C), and pH 4.5. In these experiments the gelatin concentration was high (up to 4 wt%) to avoid agglomeration of any kind. The absence of agglomeration was confirmed by the fact that no difference between the in-line turbidity measurement and that after quenching with TAI was observed. The results of Fig. 3 are in good agreement with the model that was previously developed by Leubner, Jagannathan, and Wey.<sup>2</sup>

In the case of the continuous reactor the gelatin-to-AgBr ratio was defined as an average value for the whole reactor at steady state. In the case of double-jet precipitation this ratio can only be meaningfully defined for the reaction zone around the silver reactant introduction point. This definition is

$$R_{gs} = \frac{C_g Q_t}{F_s Q_s} \quad (3)$$

where  $C_g$  is the total gelatin mass concentration in the suspension,  $F_s$  and  $Q_s$  are the molar concentration and volumetric flow rate of the silver nitrate reagent, and  $Q_t$  is the total suspension flow rate provided by the mixer at the silver reactant introduction point. As seen from the relationship of Eq. 3, by decreasing  $C_g$  and  $Q_t$  and increasing  $R$  ( $=F_s Q_s / V_t$  where  $V_t$  is the total suspension volume), a value for  $R_{gs}$  can be achieved during double-jet nucleation, such that the amount of gelatin is no longer adequate to stabilize the nuclei and agglomeration occurs. The results from such experiments after quenching with TAI will be discussed first, in order to examine the irreversible type of agglomeration.

Figure 4 shows the results of  $\log Z$  as a function  $\log R$  for  $C_g = 2$  g/L,  $Q_t = 152$  mL/sec at 40°C, pBr 2.3, and pH 4.5. This plot shows that at low  $R$  values  $Z$  increases with increasing  $R$ , as expected. However, at high values of  $R$  the trend reverses and  $Z$  decreases with increasing  $R$ , indicating the occurrence of agglomeration. Similar results were obtained at other  $C_g$  and  $Q_t$  values. Generally, the breakpoint in the  $\log Z$  versus  $\log R$  plot occurred at lower

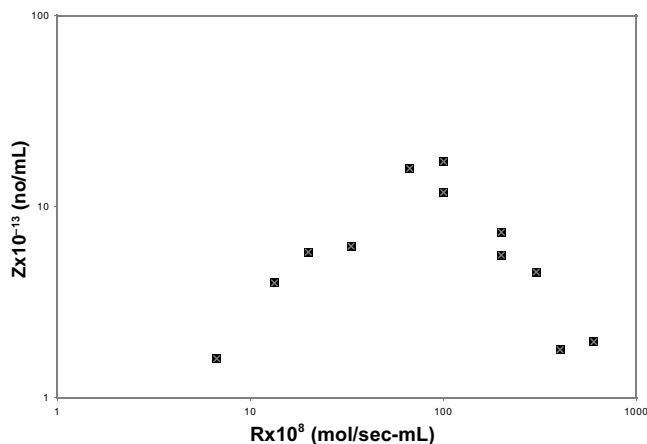


**Figure 4.** Plot of  $Z$  versus  $R$  obtained by double-jet precipitation at 40°C in the presence of low-gelatin concentration.

values of  $R$  as  $C_g$  and  $Q_t$  were decreased, as expected from the relationship of Eq. 3.

The irreversible agglomeration inferred by these experiments is concluded to occur by coalescence insofar as fast growth rates are required to reach the sizes obtained during such short times. This mechanism is supported by electron microscopy and x-ray diffraction which indicated the large particles to be monocrystalline and not aggregates.<sup>9</sup>

Calculation of  $R_{gs}$  at the breakpoint of Fig. 4, using the relationship of Eq. 3 yields a value of approximately 50 g/mol. Similar critical  $R_{gs}$  values were calculated for different combinations of  $C_g$  and  $Q_t$  values and the appropriate breakpoints in  $R$  obtained from the corresponding experiments. It is remarkable that the critical  $R_{gs}$  estimated from these double-jet experiments is identical to that obtained from the experiments with the continuous crystallizer (Figs. 1 and 2) at the same temperature. This result indicates that similar levels of gelatin are required to stabilize fine crystals of comparable size formed by these two processes.

In addition to  $C_g$ ,  $Q_t$ , and  $R$  the temperature also affected  $R_{gs}$ . Increasing the temperature above 40°C caused the breakpoints in the  $\log Z$  versus  $\log R$  curves to be shifted to larger  $R$ , reflecting smaller critical values of  $R_{gs}$ . An increase in the crystal size and a corresponding decrease in the AgBr surface area per mass at the higher temperature can account for the observed decrease in the critical  $R_{gs}$  (see Eq. 1). But the decrease in the critical  $R_{gs}$  at the higher temperature may also be attributed in part to a thicker more diffuse protective layer that inhibits coalescence.

As in the case of coalescence,  $R_{gs}$  was the most significant factor affecting flocculation. This reversible agglomeration was monitored by the difference between the sizes calculated from the turbidity measurements obtained in-line and after quenching with TAI. The extent of flocculation, denoted as  $\Delta D_f$ , was measured by the difference between the average floc diameter,  $D_f$ , and the average individual crystal diameter,  $D_i$ , generated during nucleation. A plot of  $\Delta D_f$ , as a function of  $R_{gs}$  is shown in Fig. 5. These data points were obtained with different  $C_g$ ,  $Q_t$ , and  $R$  conditions at pBr 2.3, pH 4.5, and 40°C. As seen in this plot, flocculation is evidenced below an  $R_{gs}$  value of 150 g/mol, suggesting that flocculation may be one of the steps in the coalescence mechanism, because flocculation was always present whenever coalescence was indicated by the break in the  $\log Z$  versus  $\log R$  plots.

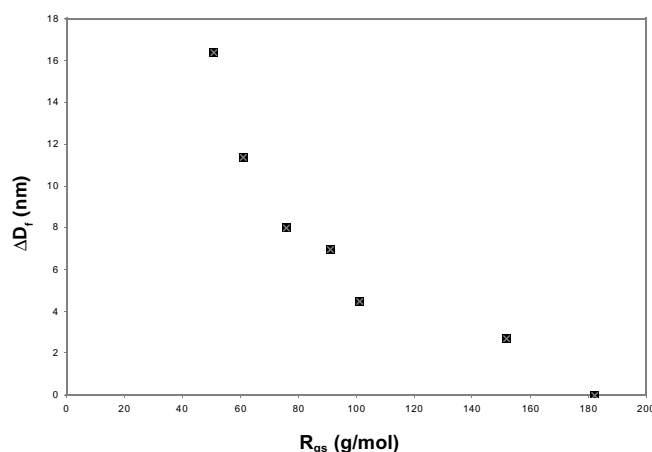


**Figure 5.** Plot of  $\Delta D_f$  versus  $R_{gs}$  for double-jet precipitation at pBr 2.3, pH 4.5, and 40°C.

Increasing the temperature reduced the propensity for flocculation, and decreasing the pBr increased the propensity for flocculation. These effects may be explained if flocculation is a result of bridging.<sup>10</sup> At higher temperatures the crystal size increases and the number ratio of gelatin molecules to AgBr particles increases, thus, restraining the bridging. But at lower pBr the increase in excess bromide ions or silver bromide complexes may reduce the number ratio of gelatin molecules to AgBr particles through an increase in the effective gelatin molecular weight, perhaps by ionic crosslinking, thus, enhancing the bridging. This mechanism also explains the absence of flocculation both at high gelatin concentrations and in gelatin-free aqueous AgBr suspensions.

Because the availability of gelatin is found to be so critical at the silver reactant introduction point, it is suggested that the gelatin-crystal association that ultimately determines the stability of the crystals occurs within a very short time domain. This gelatin-crystal association at low gelatin concentrations is probably the result of the rapidly forming crystals being forced initially to share the limited available gelatin at the reactant introduction point and is manifested as flocculation, whereas coalescence between the bridged crystals is probably attained in the bulk suspension at a slower rate. Therefore, flocculation should be a good predictor of coalescence, as is further discussed below.

### Part III. Coalescence and Tabular Grain Formation

Although the initiation of twin planes in AgBr nuclei is the key to the formation of tabular crystals, the mechanism of this event has not yet been clearly established. Several mechanisms have been proposed (see Ref. 11 for brief review), but none have been verified. Mumaw and Haugh<sup>3</sup> proposed a coalescence mechanism for the formation of twinning in silver halide crystals. The techniques for detecting flocculation and coalescence discussed above made it possible to investigate the relationship between coalescence and the formation of twinned silver bromide crystals that are suitable for growth into tabular crystals.

**Experimental.** The approach of this work was to form AgBr nuclei at double-jet precipitation conditions with a varying propensity for coalescence, and then to grow these nuclei and examine the morphology of the resulting crystals. The propensity for coalescence was monitored by the extent of flocculation during double-jet nucleation. Flocculation was

**TABLE I. Correlation Between  $\Delta D_f$  and the Tabular Grain Population at 40°C**

Gelatin concentration (g/L)	Reactant flow rate (mL/min)	$R_{gs}$ (g/mol)	$\Delta D_f$ (nm)	Tabular grain population
		<b>pBr 4.6</b>		
10	150	202	—*	Low
2	150	40	65.9	High
2	20	303	—*	Low
		<b>pBr 2.3</b>		
10	150	202	—*	Low
2	150	40	>100	High
2	20	303	5.4	Low
		<b>pBr 1.5</b>		
10	150	202	—*	Low
2	150	40	>100	High
2	20	303	>100	High

\* No statistically significant difference between  $D_i$  and  $D_p$ .

used as a measure of the coalescence propensity because of the results presented in the previous section.

The extent of flocculation during double-jet nucleation was measured, as previously, by the difference between the average floc diameter,  $D_p$ , and the average individual crystal diameter,  $D_i$ , generated during nucleation ( $\Delta D_f = D_f - D_i$ ). These measurements were made by adding to a 4.8-L agitated solution of gelatin at specified gelatin concentration, agitation rate, pBr, pH, and temperature, 100 mL of 3-M silver nitrate solution and 100 mL of a sodium bromide solution at a concentration needed to maintain the initial pBr. The two reactant solutions were added as discussed previously. The variable  $D_f$  was obtained from an in-line turbidity measurement and  $D_i$  was obtained from the turbidity after quenching with TAI, as described in Ref. 11. The experiments were repeated at various nucleation conditions known to affect flocculation and coalescence.

The twinning propensity at each nucleation condition was also examined by repeating each condition with a quarter of the reactant volumes, to reduce the number of nuclei and produce larger, more easily examined crystals during the ensuing growth. After nucleation, the gelatin concentration and pBr of each suspension were changed to the common values of 10 g/L and 1.5, respectively, to provide identical postnucleation ripening and growth conditions in all experiments. The resulting crystals were then grown at pBr 2 and 70°C as described in Ref. 11, and the tabular grain population for each condition was determined using electron microscopy. The tabular grain population was then used as an indicator of twinning propensity.

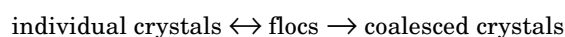
**Results and Discussion.** Because the primary variable affecting flocculation and coalescence is  $R_{gs}$ , and a variable known to affect twinning is pBr, the three main variables examined in these experiments were the gelatin concentration, the reactant flow rate, and the pBr. Table I shows the results obtained at a nucleation temperature of 40°C. The rating of the tabular grain population was done using electron micrographs of the emulsions<sup>11</sup> as follows: The tabular population was rated low if the fraction of the tabular grain projected area and the fraction of the tabular grain number in the micrographs were both below 50%, medium if the projected area was above 50% but the number below 50%, and high if both were above 50%.

As seen in Table I high and low tabular populations were produced at all nucleation pBr values, while the growth conditions were identical, revealing that the nucleation pBr is not the primary factor controlling twinning as previously believed. But a good correlation was obtained between  $\Delta D_f$ , which indicates the extent of flocculation, and

the tabular grain population which indicates the propensity for twinning. A similar correlation was obtained at a higher temperature of 70°C, with the only difference that the values of  $\Delta D_f$  were decreased, as expected from the previous results, while the tabular grain populations were decreased as well. A correlation between  $\Delta D_f$  and twinning was also obtained when the flocculation was enhanced by reducing agitation.

The results of these experiments establish a strong correlation between flocculation and twinning during nucleation, over a wide range of pBr values, de-emphasizing the effect of pBr on twinning. Nevertheless, at low-gelatin and constant- $R_{gs}$  conditions, the nucleation pBr does have an effect on the final tabular grain population, as seen in Table I. This effect of pBr on flocculation and twinning may be a result of an indirect effect of pBr on the peptizing property of gelatin as discussed earlier.

As indicated by Fig. 5, coalescence of fine AgBr crystals is always preceded by flocculation. More specifically, flocculation is probably the manifestation of a gelatin-crystal interaction resulting from the compulsory sharing of a limited amount of available gelatin by the rapidly forming nuclei. Subsequently, coalescence between the bridged crystals is probably facilitated and controlled by the initial flocculation. This mechanism may be represented by the following steps:



If the above mechanism is true, then coalescence indirectly correlates with the final tabular population and should play an important role in the twinning process.

This result raises the question of how coalescence can cause twinning. Twinning is the result of a stacking fault in the [111] plane of the AgBr rock-salt structure of the fcc lattice. To demonstrate how coalescence can produce such a stacking fault, let us consider a silver bromide nucleation event favoring coalescence. Although the nuclei appear spherical in electron micrographs, on the atomic scale they must be bounded predominantly by flat [111] and [100] faces, as these are the most stable AgBr faces. When coalescence involving [100] faces occurs, no low-energy stacking faults are expected. However, if coalescence occurs on the [111] faces, stacking faults may be obtained as follows:

Let us represent the terminating [111] layers of one of the coalescing nuclei, below the plane of coalescence, by



where the upper case designates layers of bromide ions, the lower case designates layers of silver ions, the prime

indicates the surface layer, and the letter designations refer to the rock-salt fcc stacking sequence. Then, let us consider the layers above the [111] plane of contact of a second particle coalescing with the first. To preserve charge, the surface layer of the second particle must consist of silver ions. Several stacking sequences are possible outcomes. Of these, the three lower energy sequences are:


...a B c A b C a B c' A' b C a B c A b C... (1)

...b A c B a C b A c' A' b C a B c A b C... (2)

...a C b A c B a C b' A' b C a B c A b C... (3)

Sequence 1 is the normal rock-salt fcc sequence, sequence 2 reveals a twin at  $c'$ , and sequence 3 shows a twin at  $A'$ . Therefore, of the three low-energy possibilities resulting from the coalescence of [111] planes, two have twins and one yields the normal rock-salt fcc sequence.

The correlation between  $\Delta D_f$  and the final tabular population established in this work, along with the above discussion, suggests that the measurement of  $\Delta D_f$  during

nucleation provides an excellent metric for monitoring, controlling, and generally optimizing the population of tabular crystals in tabular photographic emulsions.<sup>12</sup> Although the determination of  $\Delta D_f$  as described in the Experimental section is not comprised entirely of in-line particle size measurements, modifications may be easily made to achieve real-time determination of  $\Delta D_f$ . 

## References

1. J. S. Wey, in *Preparation and Properties of Solid State Materials*, Vol. 6, W. R. Wilcox, Ed., Marcel Dekker, New York, 1981.
2. I. H. Leubner, R. Jagannathan, and J. S. Wey, *Photogr. Sci. Eng.* **24**, 268 (1980).
3. C. T. Mumaw and E. F. Haugh, *J. Imaging Sci.* **30**, 198 (1986).
4. Y. Hosoya and S. Urabe, *Proceedings of SPSTJ Conference*, 1997; paper A-03, p. 9.
5. E. Terentev and S. Shalimova, *Proceedings of 48<sup>th</sup> IS&T Annual Conference*, 1995, p. 263.
6. M. G. Antoniadis and J. S. Wey, *J. Imaging Sci. Technol.* **36**, 517 (1992).
7. H. G. Curme and C. C. Natale, *J. Phys. Chem.* **68**, 3009 (1964).
8. M. R. V. Sahyun, *Photogr. Sci. Eng.* **20**, 92 (1976).
9. M. G. Antoniadis and J. S. Wey, *J. Imaging Sci. Technol.* **37**, 272 (1993).
10. C. A. Miller and P. Neogi, *Interfacial Phenomena*, Marcel Dekker, New York, 1985, p.119.
11. M. G. Antoniadis and J. S. Wey, *J. Imaging Sci. Technol.* **39**, 323 (1995).
12. M. G. Antoniadis, U.S. Patent 5,350,652 (1994).